

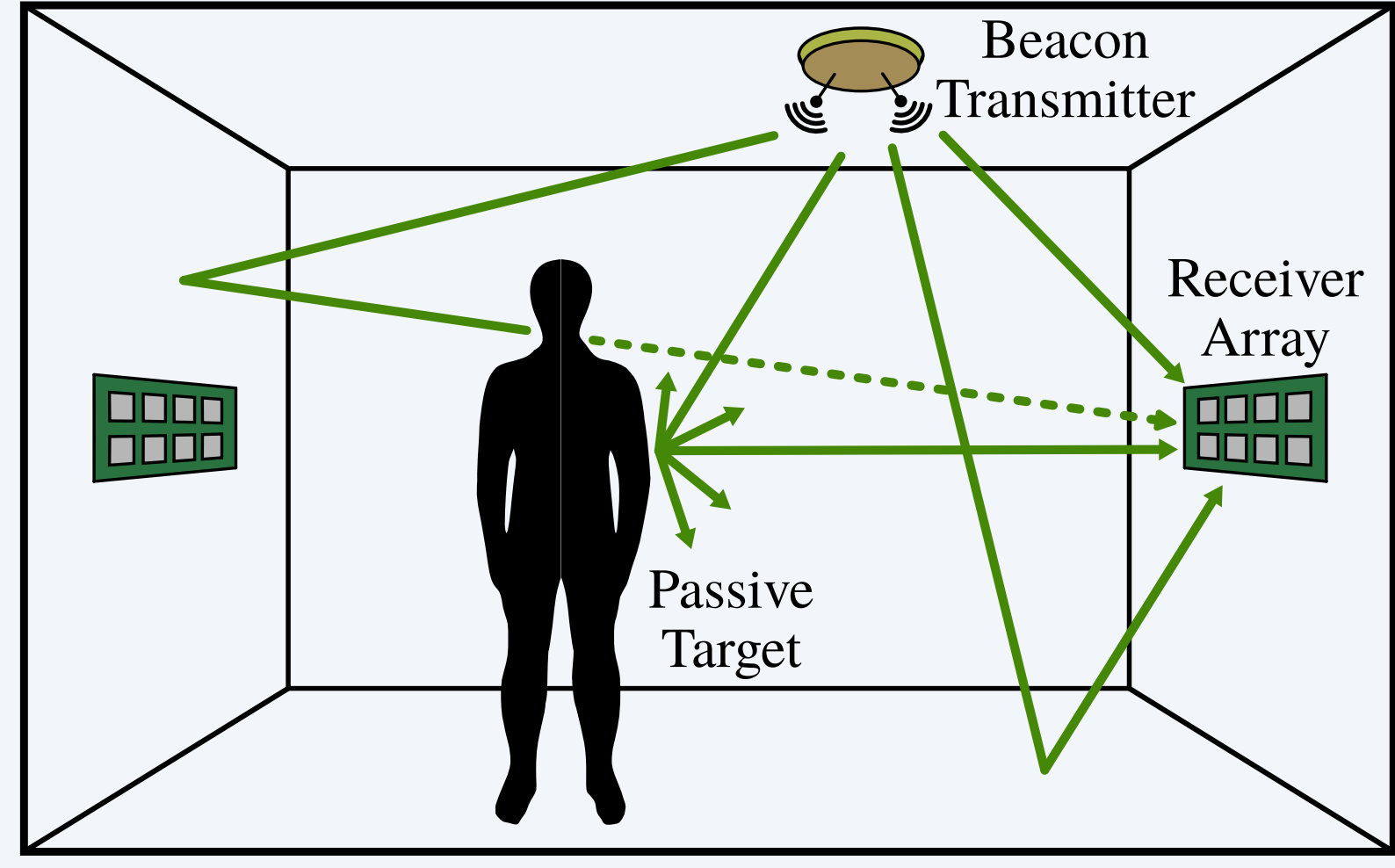
Passive Channel Charting: Locating Passive Targets using Wi-Fi Channel State Information

F. Euchner¹, D. Kellner¹, P. Stephan¹, and S. ten Brink¹

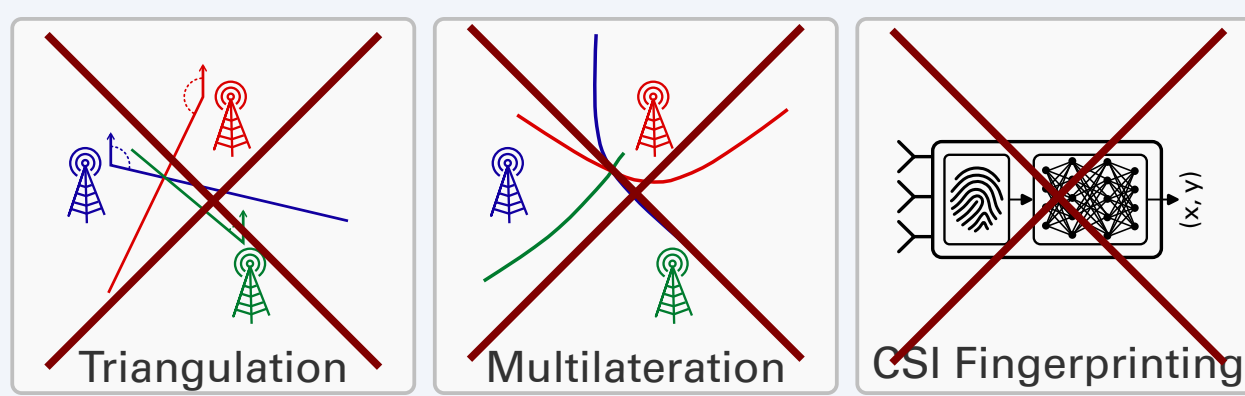
¹University of Stuttgart, Institute of Telecommunications, Pfaffenwaldring 47, 70569 Stuttgart, Germany

✉ {euchner,stephan,tenbrink}@inue.uni-stuttgart.de

Short Abstract



We propose **passive channel charting (PCC)**, an extension of **channel charting** [1] to passive targets. As in conventional channel charting, we follow a **dimensionality reduction** approach to reconstruct a physically interpretable map of target positions from similarities in high-dimensional channel state information (CSI). We evaluate our method on a CSI dataset collected indoors with a distributed setup of **ESPARGOS Wi-Fi sensing antenna arrays**. We compare PCC to a classical **triangulation** baseline and a neural network-based **fingerprinting** baseline.



PCC is **data-based**, not model-based, but model-based observations (e.g. AoA) can be taken into account! Our approach is similar to [2], now also with baselines and open code / data.

Dataset

The measured dataset \mathcal{S} is a collection of L datapoints

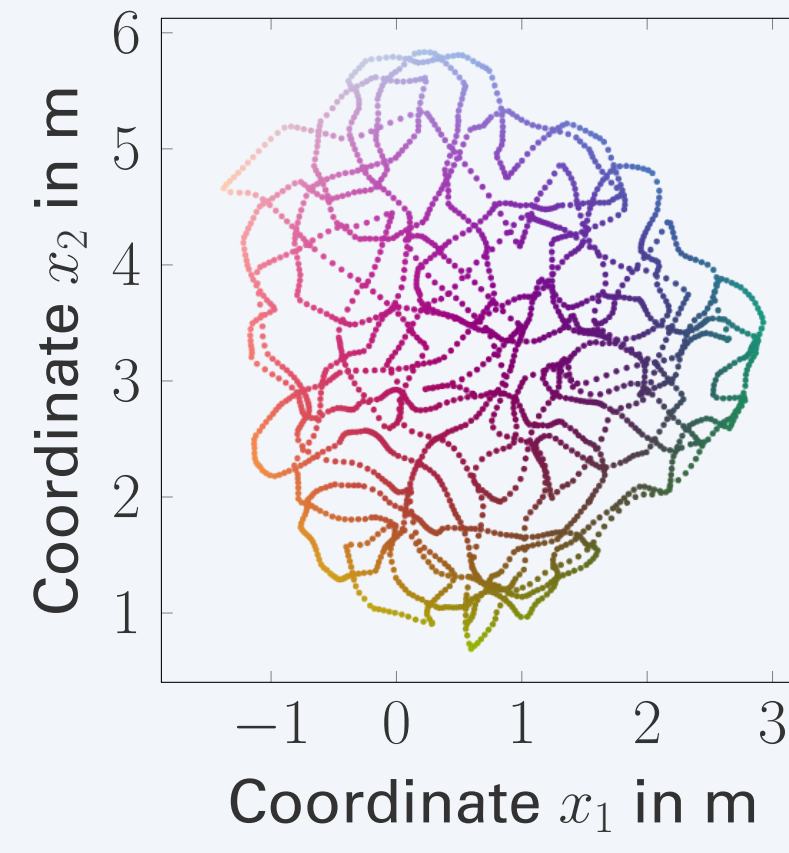
$$\mathcal{S} = \{(\mathbf{H}^{(l)}, \mathbf{x}^{(l)}, t^{(l)}, i_{\text{TX}}^{(l)})\}_{l=1, \dots, L}$$

containing frequency-domain CSI arrays $\mathbf{H}^{(l)} \in \mathbb{C}^{B \times M_r \times M_c \times N_{\text{sub}}}$, target positions $\mathbf{x}^{(l)} \in \mathbb{R}^3$, timestamps $t^{(l)} \in \mathbb{R}$ and transmitter indices $i_{\text{TX}}^{(l)} \in \{1, \dots, N_{\text{TX}}\}$.

These datasets were used:

	$\mathcal{S}_{\text{rob},\text{train}}$	$\mathcal{S}_{\text{rob},\text{test}}$	$\mathcal{S}_{\text{hum},\text{test}}$
Type	Training	Test	Test
Target	Robot	Robot	Human
L	482 882	139 427	33 011
Clusters	8 012	2 337	556

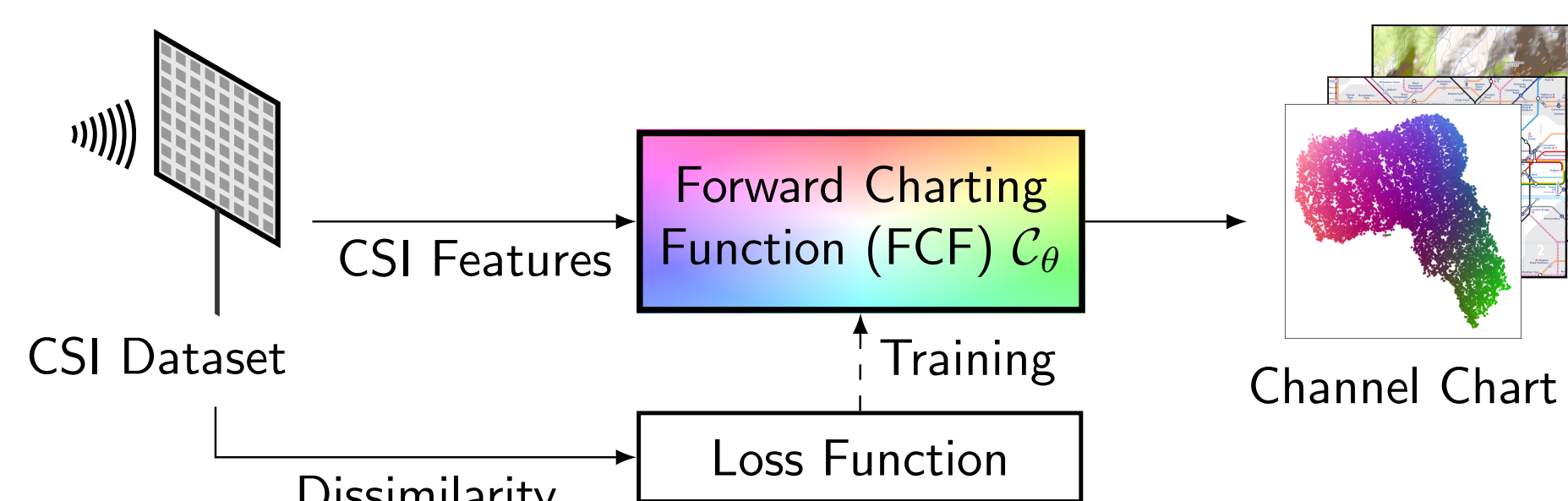
The position labels of $\mathcal{S}_{\text{rob},\text{test}}$ are shown to the right.



Preprocessing: Clutter Removal and Clustering

- First Step:** Apply Clutter Removal with Acquisitions Under Phase Noise (CRAP) algorithm [4] to remove clutter from $\mathbf{H}^{(l)}$
- Second Step:** Average all clutter-rejected datapoints in $\Delta t = 1$ s intervals into “clusters” with CSI arrays $\bar{\mathbf{H}}_{\text{tgt}}^{(l)} \in \mathbb{C}^{B \times M_r \times M_c}$

Channel Charting, Baselines and Results



Dissimilarity Metric

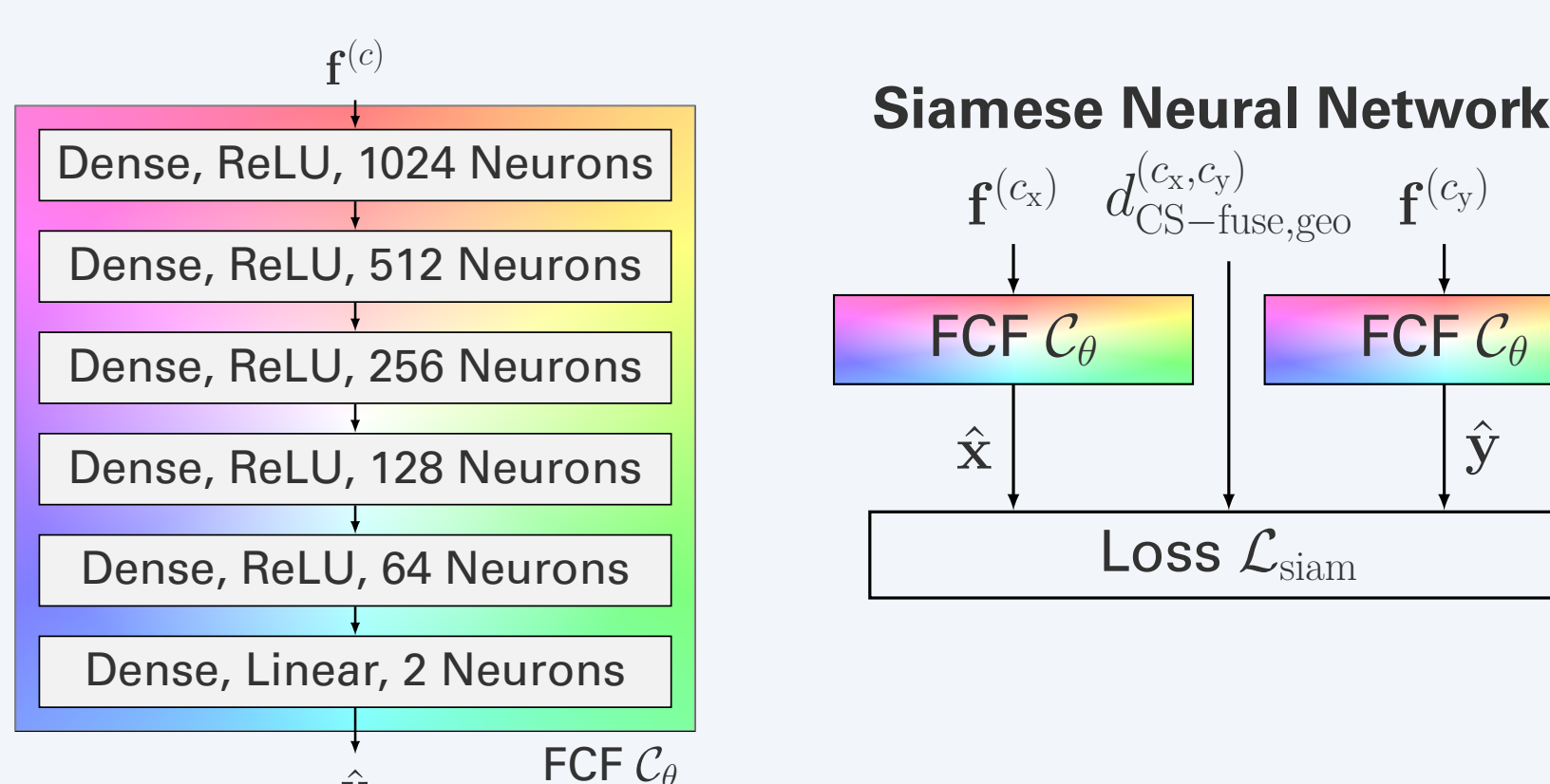
- We use a squared cosine similarity-based metric

$$d_{\text{CS}}^{(c_x, c_y)} = \sum_{b=1}^B \left(1 - \frac{\left| \sum_{m_r=1}^{M_r} \sum_{m_c=1}^{M_c} \left(\bar{\mathbf{H}}_{\text{tgt},b,m_r,m_c}^{(c_x)} \right)^* \bar{\mathbf{H}}_{\text{tgt},b,m_r,m_c}^{(c_y)} \right|^2}{\left\| \bar{\mathbf{H}}_{\text{tgt},b}^{(c_x)} \right\|_F^2 \left\| \bar{\mathbf{H}}_{\text{tgt},b}^{(c_y)} \right\|_F^2} \right),$$

to measure the dissimilarity between clusters c_x and c_y .

- Use time difference $|\bar{t}^{(c_x)} - \bar{t}^{(c_y)}|$ between clusters c_x and c_y to create a more accurate **fused dissimilarity** $d_{\text{CS-fuse}}^{(c_x, c_y)}$ [5].
- Apply shortest path algorithm [6] to obtain geodesic fused dissimilarity $d_{\text{CS-fuse,geo}}^{(c_x, c_y)}$, which is a pseudo-distance between clusters c_x and c_y .

Neural Network Training



- The forward charting function (FCF) C_θ is implemented as a dense neural network.
- Cluster-wise feature vectors $\mathbf{f}^{(c)} \in \mathbb{R}^{2 \cdot N_{\text{TX}} \cdot B \cdot N_{\text{tap}} \cdot M_r^2 \cdot M_c^2}$ based on time-domain sample autocorrelations.
- Weight-sharing Siamese neural network trained on $\mathcal{S}_{\text{rob},\text{train}}$ with Siamese loss

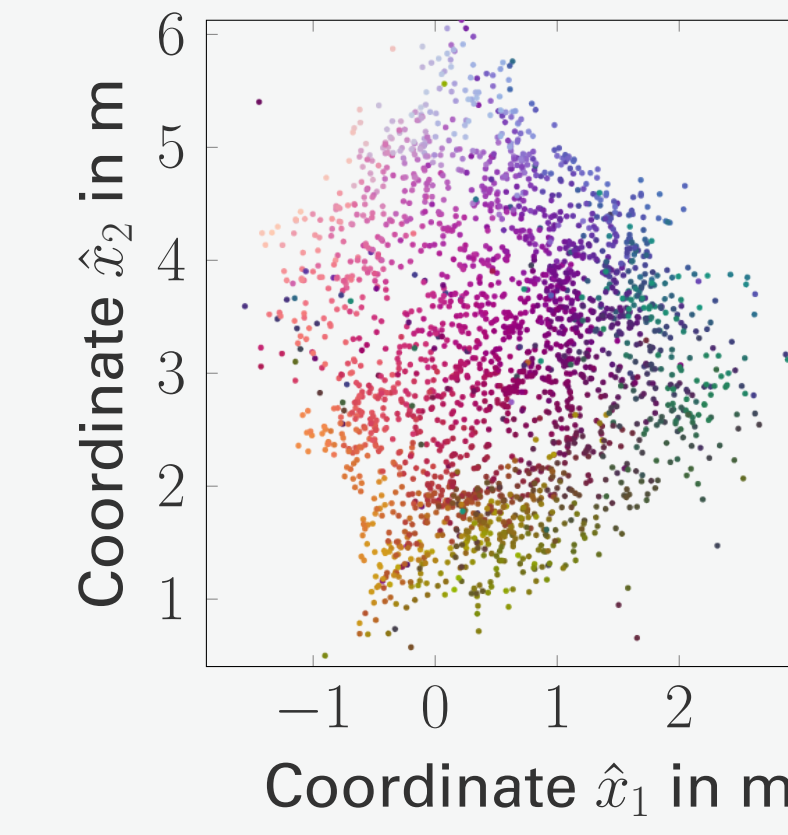
$$\mathcal{L}_{\text{siam}}^{(c_x, c_y)}(\hat{\mathbf{x}}, \hat{\mathbf{y}}) = \frac{\left(d_{\text{CS-fuse,geo}}^{(c_x, c_y)} - \|\hat{\mathbf{y}} - \hat{\mathbf{x}}\|_2 \right)^2}{d_{\text{CS-fuse,geo}}^{(c_x, c_y)} + \beta},$$

where $\hat{\mathbf{x}} = C_\theta(\mathbf{f}^{(c_x)})$ and $\hat{\mathbf{y}} = C_\theta(\mathbf{f}^{(c_y)})$ are the channel chart position predictions for the clusters c_x and c_y .

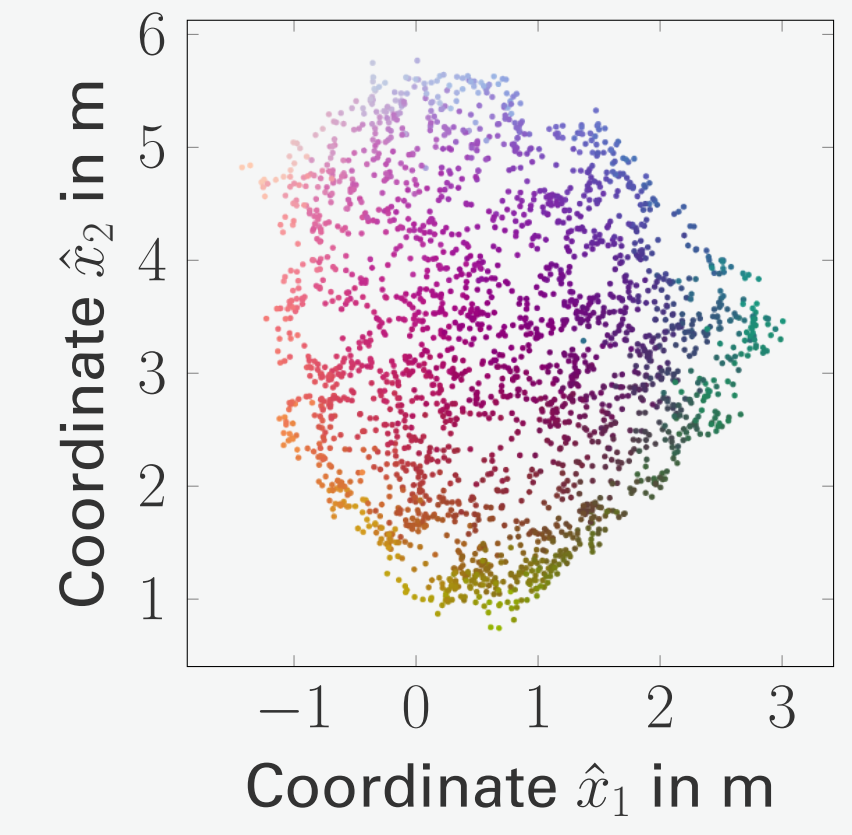
- Channel chart ideally preserves relative positions (not necessarily in physical coordinate frame).
- Augmented channel charting [7]: Augment Siamese loss with triangulation loss \mathcal{L}_{tri} : Transforms channel chart into global coordinate frame, results in FCF $C_{\theta,\text{aug}}$.

Baseline Results

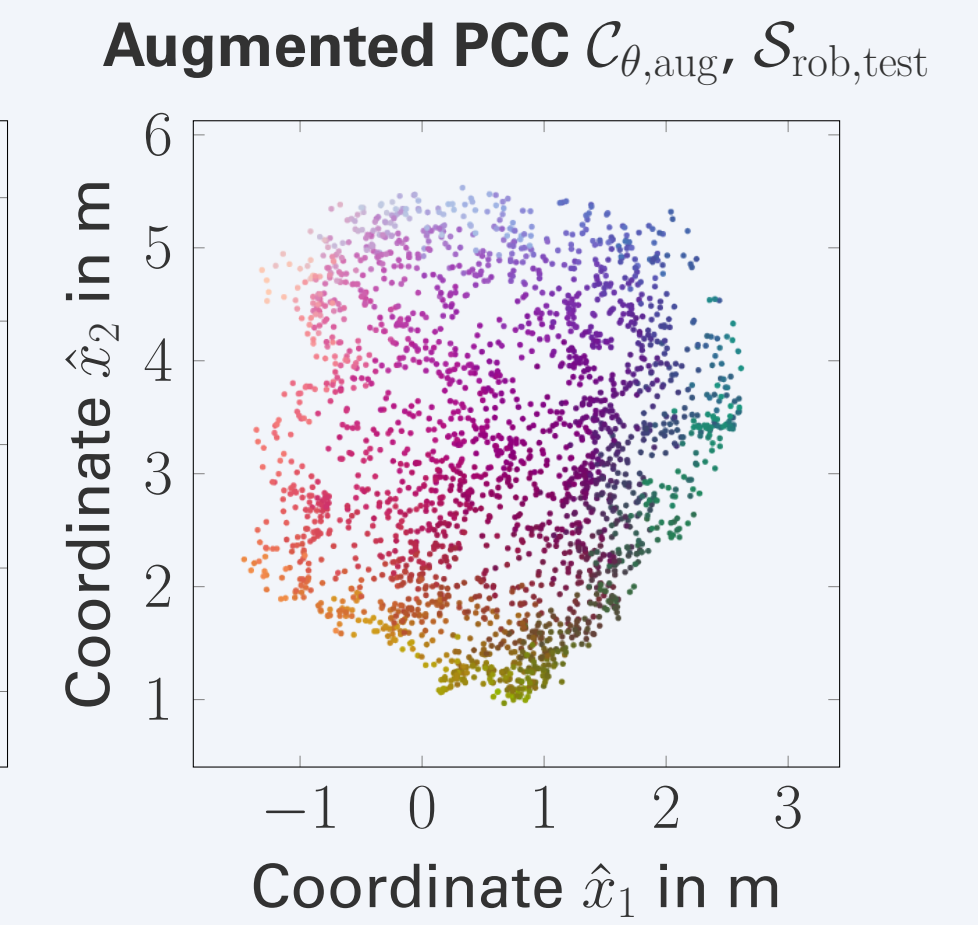
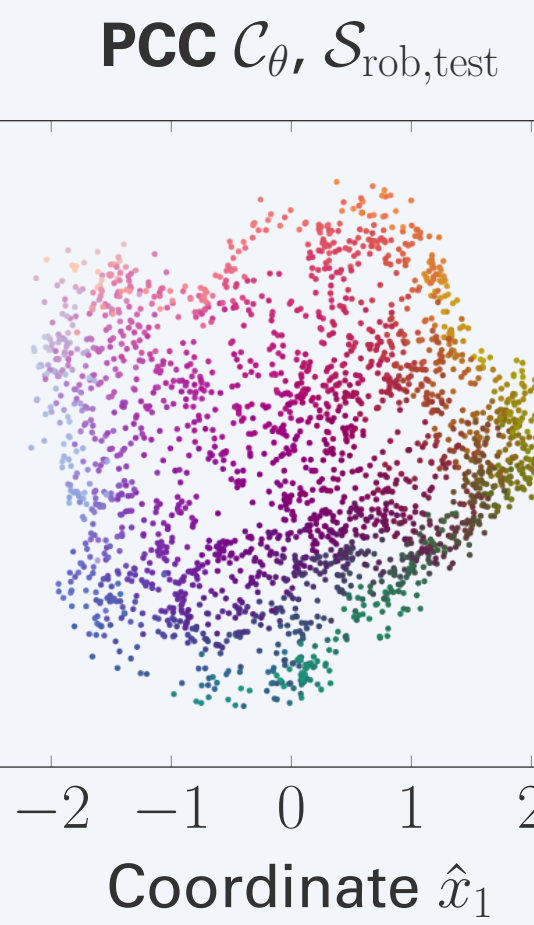
Triangulation, $\mathcal{S}_{\text{rob},\text{test}}$



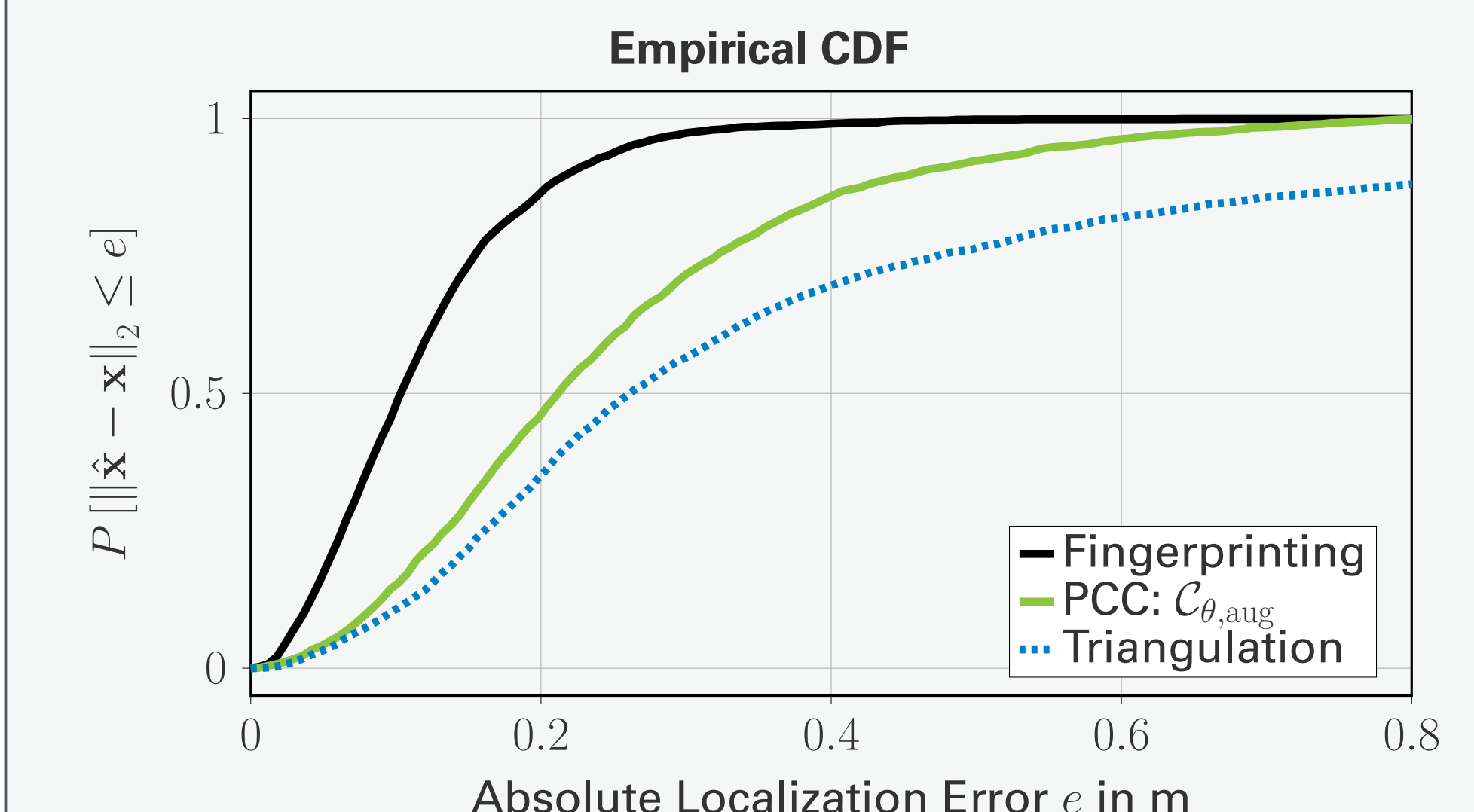
Fingerprinting, $\mathcal{S}_{\text{rob},\text{test}}$



Passive Channel Charting Results



Performance Comparison and Conclusion



Error Metric Overview, Training on $\mathcal{S}_{\text{rob},\text{train}}$

Training Set	Test Set	MED ↓	CEP ↓	R95 ↓	
Triangulation	not needed	$\mathcal{S}_{\text{rob},\text{test}}$	0.434 m	0.261 m	1.368 m
Fingerprinting	$\mathcal{S}_{\text{rob},\text{train}}$	$\mathcal{S}_{\text{rob},\text{test}}$	0.123 m	0.104 m	0.278 m
Aug. PCC $C_{\theta,\text{aug}}$	$\mathcal{S}_{\text{rob},\text{train}}$	$\mathcal{S}_{\text{rob},\text{test}}$	0.258 m	0.219 m	0.585 m
Triangulation	not needed	$\mathcal{S}_{\text{hum},\text{test}}$	0.322 m	0.227 m	0.775 m
Fingerprinting	$\mathcal{S}_{\text{rob},\text{train}}$	$\mathcal{S}_{\text{hum},\text{test}}$	0.487 m	0.311 m	1.423 m
Aug. PCC $C_{\theta,\text{aug}}$	$\mathcal{S}_{\text{rob},\text{train}}$	$\mathcal{S}_{\text{hum},\text{test}}$	0.558 m	0.370 m	1.588 m

MED = Mean Euclidean Distance, CEP = Circular Error Probable, R95 = 95th percentile error

PCC **outperforms** the classical triangulation baseline for a known target. **Challenge:** Generalization to previously unseen targets!

References

- C. Studer, S. Medjkouh, E. Gönültaş, T. Goldstein, and O. Tirkkonen, “Channel Charting: Locating Users Within the Radio Environment Using Channel State Information,” *IEEE Access*, 2018.
- I. Karmanov, F. G. Zanjani, I. Kadampot, S. Merlin, and D. Dijkman, “WiCluster: Passive Indoor 2D/3D Positioning using WiFi without Precise Labels,” in *2021 IEEE Global Communications Conference (GLOBECOM)*. IEEE, 2021.
- F. Euchner, T. Schneider, M. Gauger, and S. ten Brink, “ESPARGOS: An Ultra Low-Cost, Realtime-Capable Multi-Antenna WiFi Sounder,” in *WSA & SCC 2023: 26th International ITG Workshop on Smart Antennas and 13th Conference on Systems, Communications, and Coding*. VDE, 2023.
- M. Henninger, S. Mandelli, A. Grudnitsky, T. Wild, and S. ten Brink, “CRAP: Clutter removal with acquisitions under phase noise,” in *2nd International Conference on 6G Networking (6GNet)*. IEEE, 2023.
- P. Stephan, F. Euchner, and S. ten Brink, “Angle-Delay Profile-Based and Timestamp-Aided Dissimilarity Metrics for Channel Charting,” *IEEE Transactions on Communications*, 2024.
- M. Stahlke, G. Yammie, T. Feigl, B. M. Eskofier, and C. Mutschler, “Indoor Localization with Robust Global Channel Charting: A Time-Distance-Based Approach,” *IEEE Transactions on Machine Learning in Communications and Networking*, 2023.
- F. Euchner, P. Stephan, and S. ten Brink, “Augmenting Channel Charting with Classical Wireless Source Localization Techniques,” in *57th Asilomar Conference on Signals, Systems, and Computers*, 2023.

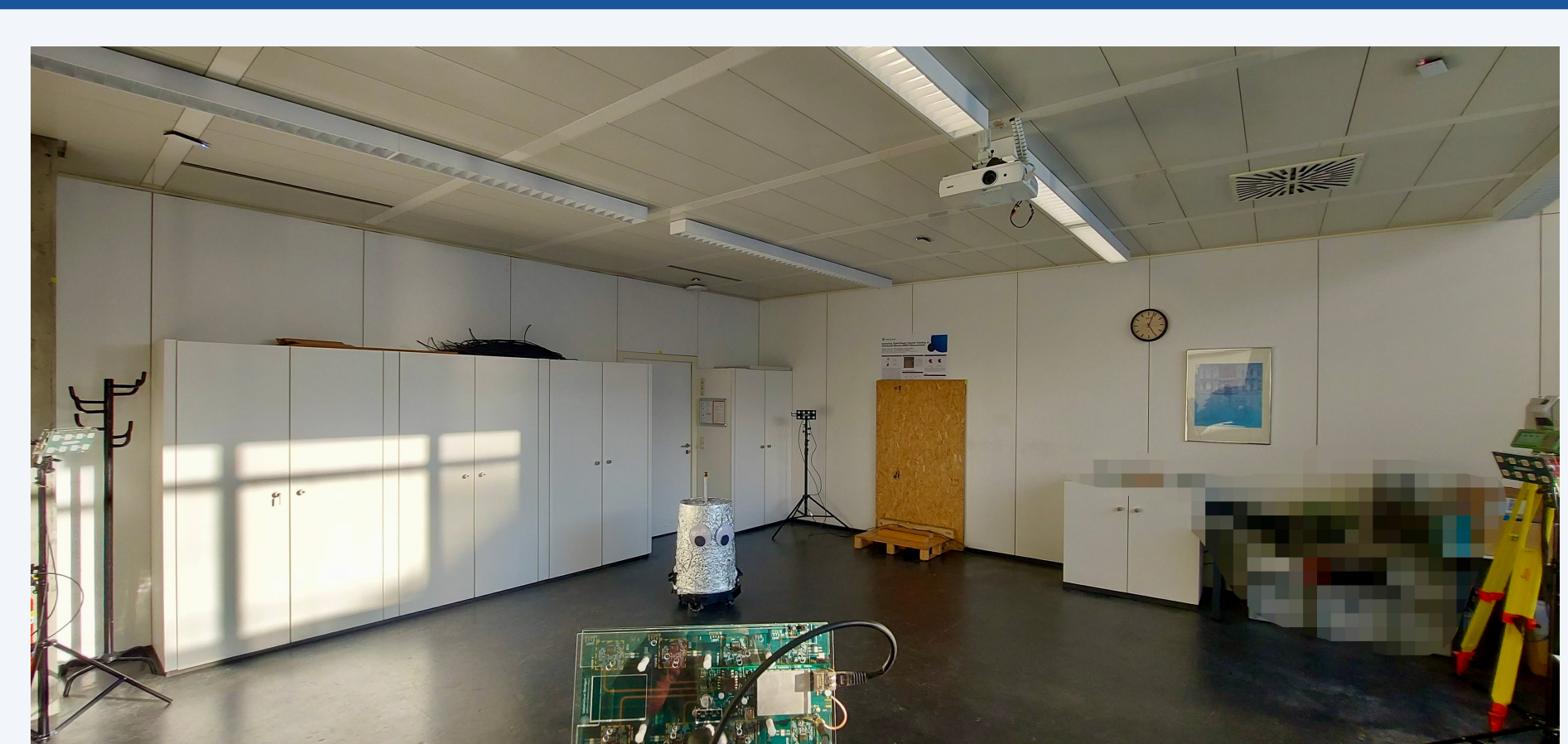
System and Experiment Setup

The ESPARGOS Antenna Array

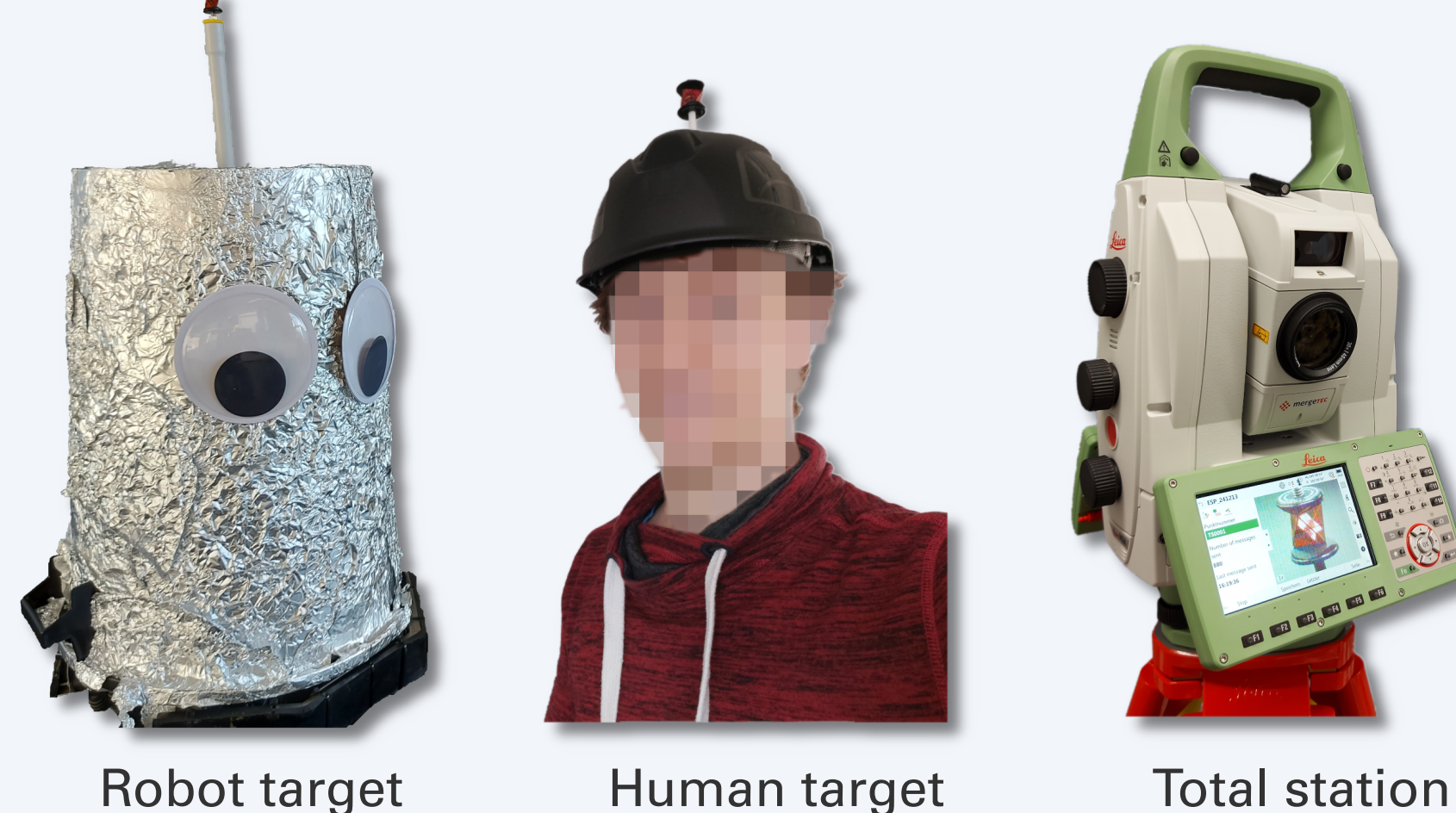


ESPARGOS [3] is a passive, ESP32-based fully-digital phased array with $M_r \times M_c = 2 \times 4$ antennas per board. It provides phase-synchronous Wi-Fi (802.11g/n) Channel State Information (CSI).

Experiment Setup / Environment



4.5 m × 4.5 m area with $B = 4$ ESPARGOS arrays, robot target



A tachymeter total station provides accurate “ground truth” position labels by tracking the laser retroreflector.

The $N_{\text{TX}} = 4$ ceiling-mounted Wi-Fi transmitters continuously broadcast Wi-Fi packets:

- $N_{\text{sub}} = 53$ nonzero subcarriers with L-LTF channel coefficients
- Carrier frequency $f_c = 2.472$ GHz, Bandwidth $W \approx 16.56$ MHz
- Approximately 60 packets per second over all transmitters